Organic LETTERS

Letter

pubs.acs.org/OrgLett

Stereoselective Synthesis, Docking, and Biological Evaluation of Difluoroindanediol-Based MenE Inhibitors as Antibiotics

Christopher E. Evans,[†] Joe S. Matarlo,[§,⊥] Peter J. Tonge,[*,§,∥] and Derek S. Tan[*,†,‡]

[†]Pharmacology Program, Weill Cornell Graduate School of Medical Sciences, and [‡]Chemical Biology Program and Tri-Institutional Research Program, Memorial Sloan Kettering Cancer Center, New York, New York 10065, United States

[§]Institute of Chemical Biology and Drug Discovery, [∥]Department of Chemistry, and [⊥]Department of Biochemistry and Cell Biology, Stony Brook University, Stony Brook, New York 11794, United States

Supporting Information

ABSTRACT: A stereoselective synthesis has been developed to provide all four side-chain stereoisomers of difluoroindanediol **2**, the mixture of which was previously identified as an inhibitor of the *o*-succinylbenzoate-CoA synthetase MenE in bacterial menaquinone biosynthesis, having promising in vitro activity against methicillin-resistant *Staphylococcus aureus* and *Mycobacterium tuberculosis*. Only the (1*R*,3*S*)-diastereomer inhibited the biochemical activity of MenE, consistent with computational docking studies, and this diastereomer also exhibited in vitro antibacterial activity comparable to that of the mixture. However, mechanism-of-action studies suggest that this inhibitor and its diastereomers may act via other mechanisms beyond inhibition of menaquinone biosynthesis.

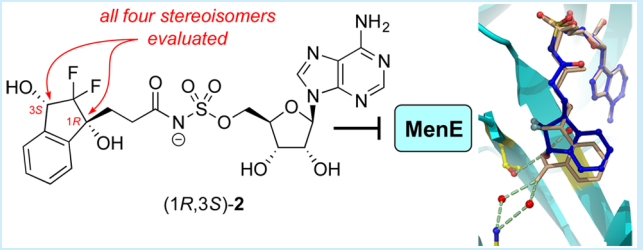

Novel antibiotics with new mechanisms of action are urgently needed to counter the growing threat of antibiotic-resistant bacterial infections.[1] Bacterial menaquinone biosynthesis is an attractive new antibacterial target.[2] Menaquinone (vitamin K_2) is a lipid-soluble electron carrier used in the electron-transport chain of cellular respiration in many bacterial species.[3] It is the sole electron carrier in Gram-positive bacteria, mycobacteria, and all anaerobically growing bacteria.[4] In contrast, humans use ubiquinone for electron transport, and although menaquinone is an important clotting factor, humans lack the de novo biosynthetic pathway for menaquinone and acquire it from diet and gut flora.[5] Menaquinone is biosynthesized in bacteria through at least nine distinct enzymes (Figure 1),[6] and inhibitors have been reported for MenD,[7] MenC,[8] MenE,[9,10] MenB,[11] and MenA.[12] The antimicrobial activity of these inhibitors corroborates genetic evidence indicating that menaquinone is essential for proliferation and survival of bacteria in which it is the sole electron carrier.[4] In particular, our laboratories have previously reported inhibitors of MenE,[9] an acyl-CoA (coenzyme A) synthetase (ligase) in the ANL (*a*cyl-CoA synthetase/*n*on-ribosomal peptide synthetase adenylation domain/*l*uciferase) family of adenylate-forming enzymes.[13] MenE catalyzes a two-step process involving initial adenylation of *o*-succinylbenzoate (OSB) to form the tightly bound OSB-AMP (adenosine 5′-monophosphate) intermediate, followed by thioesterification with CoA to form OSB-CoA.[13] We[9] and others[10] have used 5′-*O*-(*N*-acylsulfamoyl)adenosine (acyl-AMS) analogues of the tightly bound OSB-AMP reaction intermediate to target MenE. Based upon an initial inhibitor OSB-AMS (**1**), we recently discovered a difluoroindanediol analogue **2** with improved in vitro antibacterial activity against methicillin-resistant *Staphylococcus aureus* and *Mycobacterium tuberculosis* (Figure 2). The difluoroindanediol side chain was originally prepared as a mixture of four stereoisomers. Thus, to assess the activity of the individual stereoisomers, we report herein the development of a stereoselective synthesis leveraging enzymatic kinetic resolution. The individual stereoisomers of **2** were then evaluated in biochemical, computational, and cell culture studies to assess selectivity and mechanisms of action.

In our original synthesis of **2**, a racemic difluoroindanol side chain bearing a ketone at the C3 position was coupled to the AMS scaffold, with the ketone undergoing non-stereoselective reduction during a subsequent hydrogenation step.[9c] Initial efforts to resolve this racemic keto acid side chain by recrystallization with a chiral amine or chromatographic separation of corresponding chiral amine-derived diastereomeric Schiff bases were unsuccessful. Thus, to access the individual diastereomers of **2** in a stereoselective fashion, we envisioned an alternative retrosynthetic approach in which both the C1 and C3 stereocenters of the side chains **4** would be set prior to coupling to the AMS scaffold **3** (Figure 2). C1 stereochemistry would be set via diastereoselective alkyne addition to protected keto alcohol **5**, with absolute stereochemistry at C3 established in 3-hydroxy-1-indanone **6**. Notably, initial efforts to achieve stereoinduction by asymmetric reduction or alkyne addition to 2,2-difluoroindan-1,3-dione

Received: October 31, 2016
Published: December 1, 2016

DOI: 10.1021/acs.orglett.6b03272
Org. Lett. 2016, 18, 6384−6387

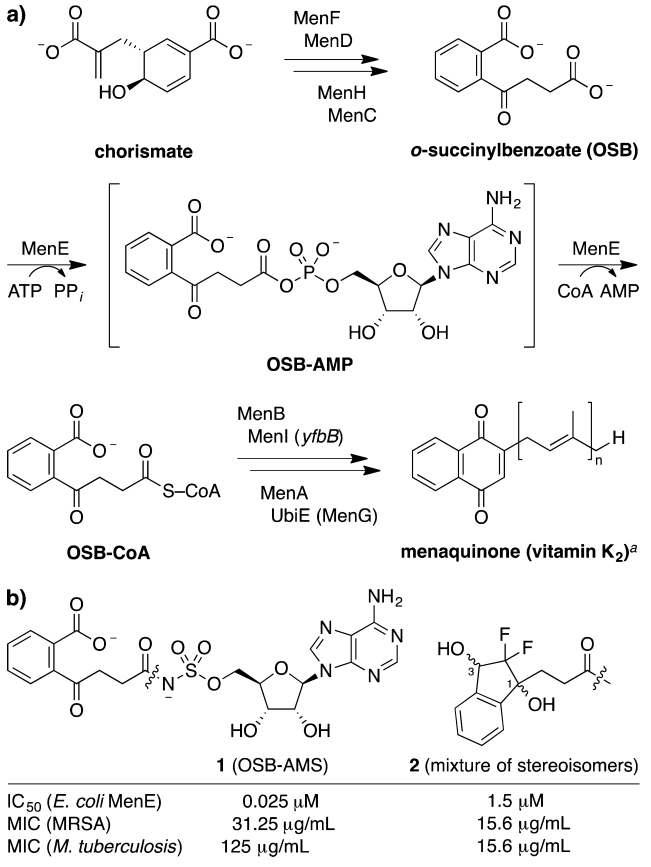

Figure 1. (a) Menaquinone biosynthetic pathway. [a]n = 4−13; n = 9 in *M. tuberculosis*; n = 8 in *S. aureus* and *E. coli*. (b) MenE inhibitors that mimic the tightly bound OSB-AMP reaction intermediate. AMP = adenosine 5′-monophosphate; ATP = adenosine 5′-triphosphate; CoA = coenzyme A; IC_{50} = 50% inhibitory concentration; MIC = minimum inhibitory concentration; MRSA = methicillin-resistant *S. aureus*; PP_i = inorganic pyrophosphate.

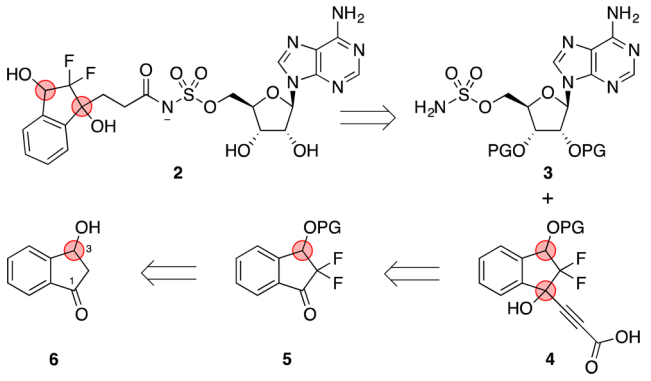

Figure 2. Stereoselective retrosynthesis of difluoroindanediol-based inhibitor **2**. PG = protecting group. Red circles indicate key stereocenters.

(not shown) yielded no enantiocontrol, perhaps due to the high reactivity of this diketone.

To access both enantiomers of 3-hydroxy-1-indanone (**6**), we carried out an enzymatic kinetic resolution with vinyl acetate and Amano Lipase PS (*Burkholderia cepacia*, formerly *Pseudomonas cepacia*), reported previously by Nair and co-workers.[14] At 50% conversion, the reaction provided the starting alcohol (3*S*)-**6** in 46% yield and >98% ee (Chiracel

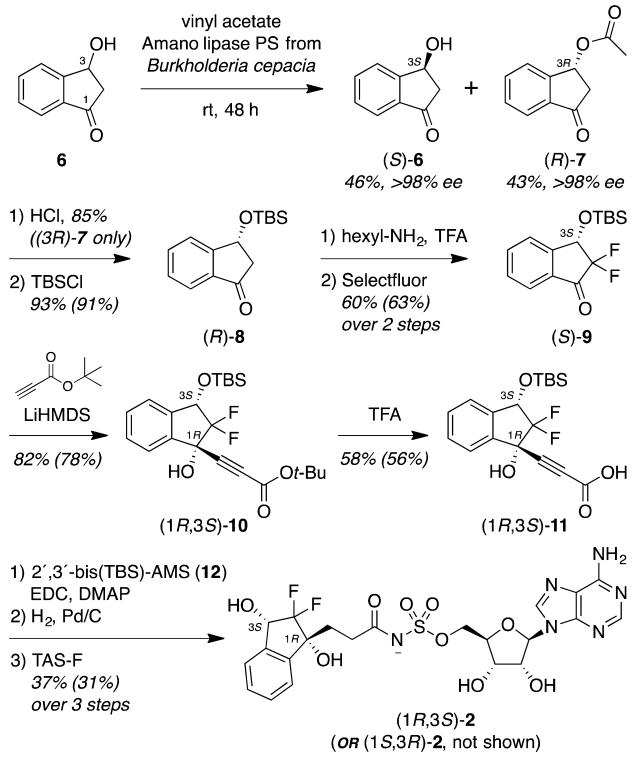

Figure 3. Synthesis of *syn*-difluoroindanediol inhibitors (1*R*,3*S*)-**2** and (1*S*,3*R*)-**2**. Yields in parentheses are for the synthesis of (1*S*,3*R*)-**2**, prepared analogously from alcohol (3*S*)-**6**. **12**: 2′,3′-bis(*tert*-butyldimethylsilyl)-5′-*O*-sulfamoyladenosine. AMS = 5′-*O*-sulfamoyladenosine; DMAP = 4-(dimethylamino)pyridine; EDC = 1-ethyl-3-(3-(dimethylamino)propyl)carbodiimide; HMDS = hexamethyldisilazide; Selectfluor =1-chloromethyl-4-fluoro-1,4-diazoniabicyclo[2.2.2]octane bis(tetrafluoroborate); TAS-F = tris(dimethylamino)sulfonium difluorotrimethylsilicate; TBS = *tert*-butyldimethylsilyl; TFA = trifluoroacetic acid.

OB-H) and the enantiomeric acetate (3*R*)-**7** in 43% yield and >98% ee, corresponding to an *E* value[15] of >200 (Figure 3).

With the C3 stereochemistry established, synthesis of the *syn*-difluoroindanediol inhibitors (1*R*,3*S*)-**2** commenced with conversion of the acetate (3*R*)-**7** to silyl ether (3*R*)-**8**.[18] Mild fluorination of the corresponding Schiff base with Selectfluor provided α-difluoroketone (3*S*)-**9**.[16] Propiolate addition under optimized conditions provided *syn*-diol (1*R*,3*S*)-**10** (>20:1 dr). The *tert*-butyl ester was cleaved, and the resulting acid was coupled to protected AMS scaffold **12**.[9] Hydrogenation of the alkyne and global deprotection provided *syn*-difluoroindanediol (1*R*,3*S*)-**2**. The other *syn*-diol diastereomer (1*S*,3*R*)-**2** was synthesized analogously from the enantiomeric alcohol (3*S*)-**6**. Absolute and relative stereochemistry were confirmed by X-ray crystallographic analysis (CuKα radiation for determination of absolute configuration[17]) of the diol obtained via desilylation of silyl ether (1*S*,3*R*)-**11**.[18]

To access the corresponding *anti*-difluorindanediol inhibitor (1*R*,3*R*)-**2**, we used an oxidation/re-reduction approach starting from protected *syn*-diol intermediate (1*R*,3*S*)-**10** to afford *anti*-diol acid (1*R*,3*R*)-**15** (Figure 4). The intermediate *anti*-diol ester (1*R*,3*R*)-**14** exhibited a diagnostic ^{1}H NMR shift of 5.41 ppm for C3-H, compared to 5.11 ppm for the epimeric *syn*-diol ester (1*R*,3*S*)-**14** obtained after the initial desilylation of (1*R*,3*S*)-**10**.[18] The enantiomeric excess was also confirmed for all four diastereomeric diol esters **14** by chiral HPLC analysis

DOI: 10.1021/acs.orglett.6b03272
Org. Lett. 2016, 18, 6384−6387

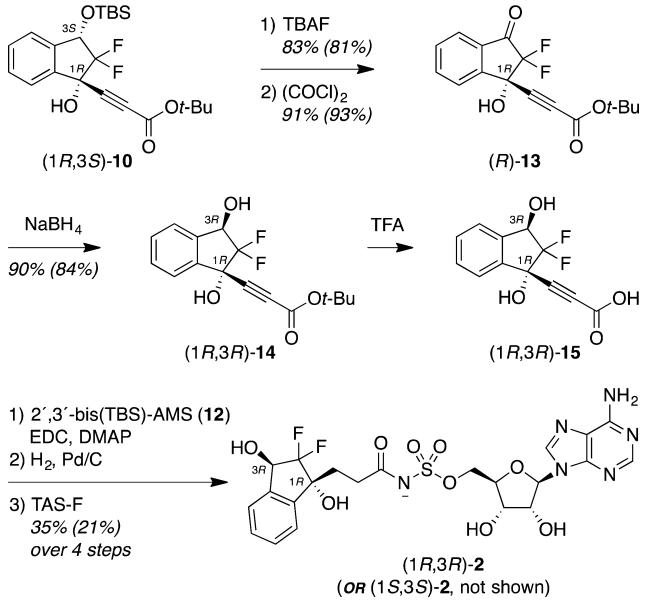

Figure 4. Synthesis of *anti*-difluoroindanediol inhibitors (1*R*,3*R*)-**2** and (1*S*,3*S*)-**2**. Yields in parentheses are for synthesis of (1*S*,3*S*)-**2**. TBAF = tetrabutylammonium fluoride.

(>98% ee),[18] ruling out possible racemization at earlier stages of the synthesis (**6** → **10**, Figure 3). Coupling of *anti*-diol acid (1*R*,3*R*)-**15** to protected AMS scaffold **12**, alkyne hydrogenation, and global deprotection afford *anti*-difluoroindanediol (1*R*,3*R*)-**2**. The other *anti*-diol diastereomer (1*S*,3*S*)-**2** was synthesized analogously from the enantiomeric protected *syn*-diol intermediate (1*S*,3*R*)-**10**.

Next, we carried out computational docking (Glide, Schrödinger) using our recently reported cocrystal structure of *E. coli* MenE (R195K mutant) in complex with OSB-AMS (**1**) (Figure 5 and Figure S1).[9c,18] Docking of OSB-AMS into the protein provided a ligand pose well-aligned with that observed in the cocrystal structure (rmsd 0.2 Å).[18] In docking of the four diastereomeric difluoroindanediols **2**, the adenosine region of each diasteromer bound in an orientation consistent with that of OSB-AMS, retaining key interactions and filling the adenosine binding pocket. However, in the side-chain region, only the *syn*-difluoroindanediol (1*R*,3*S*)-**2** filled the binding OSB pocket fully, overlapping well with the OSB aromatic ring of cocrystallized OSB-AMS. The secondary alcohol of the difluoroindanediol appeared poised to engage in hydrogen bonding with a conserved water H_2O-666 and the alcohol side chain of Thr-277, which both interact with the OSB carboxylate in cocrystallized OSB-AMS.[9c]

Notably, in earlier docking studies with unliganded *S. aureus* MenE,[9b] we identified a Ser-302 side chain (Thr-178 in *M. tuberculosis*) that could interact with the OSB ketone of OSB-AMS. Although this alcohol side chain is absent in *E. coli* MenE (Gly-268), the docking studies herein suggest that the tertiary alcohol of the difluoroindanediol in (1*R*,3*S*)-**2** may be positioned to interact with this side chain in *S. aureus* and *M. tuberculosis* MenE.

We next tested the biochemical inhibitory activity of the four diastereomeric difluoroindanediols **2** against *E. coli* MenE (Table 1).[9,18] Consistent with the results of the docking studies above, the *syn*-difluoroindanediol (1*R*,3*S*)-**2** was the most potent inhibitor (entry 2), while none of the other three diastereomers inhibited the enzyme at up to 200 μM

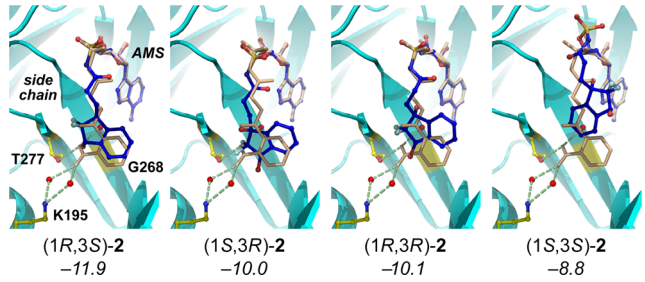

Figure 5. Computational docking of diastereomeric difluoroindanediols **2** (blue) to *E. coli* MenE R195K (cyan) (PDB: 5C5H), overlaid with co-crystallized OSB-AMS (beige), with key binding residues (yellow) and conserved waters (red). Schrödinger Glide docking scores shown for each diastereomer (arbitrary units).[18] OSB-AMS docked with a score of −13.9 (Figure S1).[18]

concentration (entries 3−5). The (1*R*,3*S*)-**2** diastereomer was also approximately 4-fold more potent than the mixture of all four diastereomers **2** (entry 1), suggesting that this single diastereomer is responsible for the observed inhibitory activity of the mixture.

We then evaluated the antimicrobial activity of the difluoroindanediols **2** against *Bacillus subtilis*, methicillin-resistant *S. aureus* (MRSA), and *M. tuberculosis* (Table 1).[18] Surprisingly, all four individual diastereomers exhibited MIC (minimum inhibitory concentration) values similar to that of the mixture of diasteromers. When the cultures were complemented with exogenous menaquinone-4, a 4-fold increase in MIC values was observed for the mixture of diastereomers (entry 1), while 2- to 4-fold increases were also observed for the MenE inhibitor (1*R*,3*S*)-**2** (entry 2), consistent with a mechanism of action involving inhibition of menaquinone biosynthesis. Some rescue was also observed for the other *syn*-diastereomer (1*S*,3*R*)-**2** in *B. subtilis* and *M. tuberculosis* (entry 3), while no rescue was observed for the *anti* diastereomers (entries 4 and 5). This suggests that the antimicrobial activity of the last three diastereomers results from other mechanisms of action, consistent with their lack of biochemical activity against MenE.

Finally, we evaluated the effects of the inhibitors on menaquinone biosynthesis in MRSA by LC-MS/MS.[9c] MRSA treated with OSB-AMS (**1**) showed a statistically significant 2.5-fold decrease in menaquinone-8, consistent with our previously published findings (Figure S2).[9c,18] The mixture of four diastereomers **2** also elicited a smaller, but statistically significant, 31% decrease in menaquinone-8. However, none of the individual difluoroindanediol diastereomers caused a significant decrease in menaquinone-8. Taken together, these results suggest that even the MenE inhibitor (1*R*,3*S*)-**2** may act via mechanisms other than inhibition of menaquinone biosynthesis.

In conclusion, we have developed a stereoselective synthesis of all four diastereomers of a difluoroindanediol-based inhibitor of MenE. Enzymatic kinetic resolution was used to establish absolute stereochemistry, and diastereoselective transformations were used to set relative stereomchemistry. Biochemical and docking studies identified the *syn*-diastereomer (1*R*,3*S*)-**2** as an effective MenE inhibitor that may engage in active-site interactions similar to those observed for the reaction intermediate analogue OSB-AMS (**1**). However, microbiological experiments suggest that (1*R*,3*S*)-**2** may have multiple mechanisms of action beyond inhibition of bacterial menaqui-

DOI: 10.1021/acs.orglett.6b03272
Org. Lett. 2016, 18, 6384−6387

Table 1. Biochemical and Antimicrobial Activity of Diastereomeric Difluoroindanediols 2

entry	inhibitor	MenE IC_{50}[a] (μM)	*B. subtilis* MIC[b] (μg/mL)	MRSA MIC[b] (μg/mL)	*M. tuberculosis* MIC[b] (μg/mL)
1	**2**[c]	18.3 ± 3.7[d]	15.6 (62.5)	15.6 (62.5)	15.6 (62.5)
2	(1*R*,3*S*)-**2**	5.0 ± 1.0	15.6 (31.2)	15.6 (31.2)	15.6 (62.5)
3	(1*S*,3*R*)-**2**	>200	15.6 (31.2)	31.2 (31.2)	31.2 (62.5)
4	(1*R*,3*R*)-**2**	>200	15.6 (15.6)	15.6 (15.6)	15.6 (31.2)
5	(1*S*,3*S*)-**2**	>200	15.6 (15.6)	15.6 (15.6)	31.2 (31.2)
6	AMS[e]	nd[f]	3.9 (3.9)	1.9 (1.9)	0.16 (0.32)

[a]*E. coli* MenE.[18] [b]MIC values in parentheses determined with addition of exogenous menaquinone-4 (10 μg/mL). [c]Equimolar mixture of four diastereomers, prepared by the original synthetic route.[9c] [d]This IC_{50} is higher than the 1.5 μM that we reported previously[9c] due to batch-to-batch variability of the enyzme preparation; IC_{50} values reported herein were all determined with the same batch of enzyme preparation. [e]5′-*O*-Sulfamoyladenosine. [f]nd = not determined.

none biosynthesis. Efforts to optimize this inhibitor and to probe its mechanism of action are ongoing.

■ ASSOCIATED CONTENT

Supporting Information

The Supporting Information is available free of charge on the ACS Publications website at DOI: 10.1021/acs.orglett.6b03272.

X-ray crystallographic data for (1*S*,3*R*)-**15** (CIF)
Experimental procedures and analytical data for all new compounds (PDF)

■ AUTHOR INFORMATION

Corresponding Authors

*E-mail: peter.tonge@stonybrook.edu.
*E-mail: tand@mskcc.org.

ORCID

Christopher E. Evans: 0000-0001-9777-4114

Notes

The authors declare the following competing financial interest(s): The authors are co-inventors of a patent application based on this work.

■ ACKNOWLEDGMENTS

We thank Dr. Stephen Walker (Stony Brook University) for assistance with BSL2 and cell culture studies, Dr. Robert Rieger (Stony Brook University Proteomics Center) for assistance with MK quantification and analysis, Dr. George Sukenick, Rong Wang, Dr. Hui Liu, Hui Fang, and Dr. Sylvi Rusli (MSKCC) for expert NMR and mass spectrometry support, and Dr. Kristin Kirschbaum and Kelly Lambright (University of Toledo) for X-ray crystallographic analysis. Financial support from the NIH (R01 GM100477 to D.S.T., R01 GM102864 to P.J.T., T32 GM073546-Gross to C.E.E., and Cancer Center Support Grant P30 CA008748 to C. B. Thompson) and a W. Burghardt Turner Fellowship (to J.S.M.) is gratefully acknowledged.

■ REFERENCES

(1) (a) Silver, L. L. *Clin. Microbiol. Rev.* **2011**, *24*, 71−109. (b) Fischbach, M. A.; Walsh, C. T. *Science* **2009**, *325*, 1089−1093. (c) Koul, A.; Arnoult, E.; Lounis, N.; Guillemont, J.; Andries, K. *Nature* **2011**, *469*, 483−490.

(2) (a) Kurosu, M.; Begari, E. *Molecules* **2010**, *15*, 1531−1553. (b) Meganathan, R. In *Comprehensive Natural Products II*; Elsevier: Oxford, 2010; pp 411−444.

(3) (a) Kurosu, M.; Begari, E. *Molecules* **2010**, *15*, 1531−1553. (b) Meganathan, R. In *Comprehensive Natural Products II*; Elsevier: Oxford, 2010; pp 411−444.

(4) (a) Collins, M. D.; Goodfellow, M.; Minnikin, D. E. *J. Gen. Microbiol.* **1979**, *110*, 127−136. (b) Nahaie, M. R.; Goodfellow, M.; Minnikin, D. E.; Hajek, V. *J. Gen. Microbiol.* **1984**, *130*, 2427−2437. (c) Hiratsuka, T.; Furihata, K.; Ishikawa, J.; Yamashita, H.; Itoh, N.; Seto, H.; Dairi, T. *Science* **2008**, *321*, 1670−1673.

(5) Dowd, P.; Ham, S.-W.; Naganathan, S.; Hershline, R. *Annu. Rev. Nutr.* **1995**, *15*, 419−440.

(6) (a) Meganathan, R. In *Vitamins and Hormones*; Litwack, G., Ed.; Academic Press, 2001; Vol. *61*, pp 173−218. (b) Truglio, J. J.; Theis, K.; Feng, Y.; Gajda, R.; Machutta, C.; Tonge, P. J.; Kisker, C. *J. Biol. Chem.* **2003**, *278*, 42352−42360. (c) Upadhyay, A.; Fontes, F. L.; Gonzalez-Juarrero, M.; McNeil, M. R.; Crans, D. C.; Jackson, M.; Crick, D. C. *ACS Cent. Sci.* **2015**, *1*, 292−302.

(7) Fang, M.; Toogood, R. D.; Macova, A.; Ho, K.; Franzblau, S. G.; McNeil, M. R.; Sanders, D. A. R.; Palmer, D. R. J. *Biochemistry* **2010**, *49*, 2672−2679.

(8) Pulaganti, M.; Banaganapalli, B.; Mulakayala, C.; Chitta, S. K.; C. M., A. *Appl. Biochem. Biotechnol.* **2014**, *172*, 1407−1432.

(9) (a) Lu, X.; Zhang, H.; Tonge, P. J.; Tan, D. S. *Bioorg. Med. Chem. Lett.* **2008**, *18*, 5963−5966. (b) Lu, X.; Zhou, R.; Sharma, I.; Li, X.; Kumar, G.; Swaminathan, S.; Tonge, P. J.; Tan, D. S. *ChemBioChem* **2012**, *13*, 129−136. (c) Matarlo, J. S.; Evans, C. E.; Sharma, I.; Lavaud, L. J.; Ngo, S. C.; Shek, R.; Rajashankar, K. R.; French, J. B.; Tan, D. S.; Tonge, P. J. *Biochemistry* **2015**, *54*, 6514−6524.

(10) Tian, Y.; Suk, D.-H.; Cai, F.; Crich, D.; Mesecar, A. D. *Biochemistry* **2008**, *47*, 12434−12447.

(11) (a) Li, X.; Liu, N.; Zhang, H.; Knudson, S. E.; Slayden, R. A.; Tonge, P. J. *Bioorg. Med. Chem. Lett.* **2010**, *20*, 6306−6309. (b) Li, X.; Liu, N.; Zhang, H.; Knudson, S. E.; Li, H.-J.; Lai, C.-T.; Simmerling, C.; Slayden, R. A.; Tonge, P. J. *ACS Med. Chem. Lett.* **2011**, *2*, 818−823. (c) Matarlo, J. S.; Lu, Y.; Daryaee, F.; Daryaee, T.; Ruzsicska, B.; Walker, S. G.; Tonge, P. J. *ACS Infect. Dis.* **2016**, *2*, 329−340.

(12) Kurosu, M.; Crick, D. C. *Med. Chem.* **2009**, *5*, 197−207.

(13) (a) Meganathan, R.; Bentley, R. *J. Bacteriol.* **1979**, *140*, 92−98. (b) Kwon, O.; Bhattacharyya, D. K.; Meganathan, R. *J. Bacteriol.* **1996**, *178*, 6778−6781.

(14) Joly, S.; Nair, M. S. *Tetrahedron: Asymmetry* **2001**, *12*, 2283−2287.

(15) Chen, C. S.; Fujimoto, Y.; Girdaukas, G.; Sih, C. J. *J. Am. Chem. Soc.* **1982**, *104*, 7294−7299.

(16) Sletten, E. M.; Nakamura, H.; Jewett, J. C.; Bertozzi, C. R. *J. Am. Chem. Soc.* **2010**, *132*, 11799−11805.

(17) The Flack parameter was determined from Parsons' quotients to be −0.03(5) using a Bruker Apex Duo diffractometer equipped with an ImuS CuKa radiation source (1.54178 Å), indicating the correct absolute configuration.

(18) See the Supporting Information for complete details.

DOI: 10.1021/acs.orglett.6b03272
Org. Lett. 2016, 18, 6384−6387